Environmental Science
Water Research & Technology

Prediction of organic groundwater contaminants degradation during medium pressure UV/NO3- treatment

Journal:	*Environmental Science: Water Research & Technology*
Manuscript ID	EW-ART-02-2023-000102.R2
Article Type:	Paper

Water Impact Statement

Groundwater contamination pose a global concern to drinking water quality. An attractive treatment alternative is the combination of UV light and indigenous NO_3^-, which generates radicals and act as a chemical-free advanced oxidation. Here we demonstrate UV/NO_3^- degradation of important groundwater contaminants, using a medium pressure Hg lamp. Furthermore, we present simple metrics to predict the UV/NO_3^- degradability of contaminants.

Prediction of organic groundwater contaminants degradation during medium pressure UV/NO_3^- treatment

Lidori Edri[a], Karl G Linden[b], Nadeem Ibrahim[a], Dror Avisar[c], Aviv Kaplan[c], Sarah Hayoune[a], Yaal Lester[a*]

[a] Environmental Technologies, Department of Materials Engineering, Azrieli College of Engineering, Jerusalem 9103501, Israel

[b] Department of Civil, Environmental, and Architectural Engineering, University of Colorado Boulder, Boulder, Colorado 80303, United States

[c] The Water Research Center, Porter School for Environment and Earth Sciences, Faculty of Exact Sciences, Tel Aviv University, Tel Aviv 69978, Israel; avivkaplan@tauex.tau.ac.il

Abstract

Irradiation of nitrate (NO_3^-) with UVC light below 240 nm generates photo-sensitized oxidants, such as hydroxyl radicals (•OH) and reactive nitrogen species (RNS). Hence, the combination UV/NO_3^- can be regarded as an advanced oxidation treatment of wastewater and groundwater, using indigenous NO_3^- to promote radicals and degrade contaminants. The present study demonstrates UV/NO_3^- degradation of important groundwater contaminants, using a polychromatic medium pressure Hg lamp. Compounds were divided into groups, based on their UV/NO_3^- degradation kinetics and photochemical parameters: Photo-reactive and photo-stable, and slow and fast reaction with radicals. Two metrics were proposed to determine the photosensitivity of a contaminant: fluence-based rate constants (k_{UV}, cm^2/mJ) and the product of

molar absorption coefficient around 223 nm and photolysis quantum yield (ε_{223} x Φ), with thresholds separating low and high values of 2 x10^{-4} cm^2/mJ and 4 l/cm/E respectively. Radicals reactivity was determined using $k_{\bullet OH,C}$,with 1x10^9 $M^{-1}s^{-1}$ as the cutoff between slow to fast reacting contaminants. NO_3^- at concentrations ≤ 5 mg/L - N enhanced UV degradation of photo-stable compounds with fast •OH reaction, due to NO_3^- dominant role as radicals' promoter. At higher NO_3^- concentrations, degradation rate stabilized or even decreased, due to the formation of NO_2^-, an •OH scavenger. For compounds with low •OH reaction, the presence of NO_3^- (up to 15 mg/L-N) either slowed their degradation rate or did not affect their UV degradation. Only contaminants with a high range of reactivity will be significantly degraded by UV/NO_3^-, without generating levels of NO_2^- above regulatory thresholds. These include contaminants with $k_{\bullet OH,C}$ > 8x10^9 $M^{-1}s^{-1}$ and contaminants with $k_{\bullet OH,C}$ > 1x10^9 $M^{-1}s^{-1}$ and k_{UV} > 5 x10^{-4} cm^2/mJ or ε_{223} x Φ > 10 l/cm/E. A simplified decision tree was proposed to predict the degradability of a contaminant during UV/NO_3^- groundwater treatment.

Keywords: Advanced oxidation, nitrate, groundwater, medium pressure, UV treatment

INTRODUCTION

Photosensitization of nitrate (NO_3^-) by UV and solar light generates hydroxyl radicals (•OH), reactive nitrogen species – RNS (e.g nitrogen dioxide •NO_2) and other intermediates (1–4). These oxidants may react with organic compounds in water, contributing to their degradation and lifetime in the environment (3). In addition, the combination of UV light and NO_3^- can be regarded as an advanced oxidation process (AOP), degrading organic contaminants during water and wastewater treatments (5). In this case, water containing indigenous NO_3^- and organic contaminants is treated

with UV light, at wavelengths overlapping NO_3^- absorption peak (principally $\lambda < 240$ nm), using for example polychromatic medium pressure (MP) mercury vapor lamp or KrCl* excimer lamp at 222 nm (6), and the photo-produced oxidants degrade any target contaminants.

The combination UV/NO_3^- was first proposed as a wastewater treatment in 2012 by Linden and his coworkers (5), which showed that irradiation of NO_3^- (> 5 mg/L-N) with an MPUV lamp generates similar •OH concentration as irradiating 10 mg/L H_2O_2 (the well-known UV/H_2O_2). Their results were later validated by Lester et al. (7), using a pilot-scale wastewater treatment system. In this case, degradation rates of different contaminants by MPUV/NO_3^- (using native NO_3^-) were comparable to their degradation by LPUV/H_2O_2. More recently, Lester and his group demonstrated the potential of MPUV/NO_3^- to degrade 1,4-dioxane, a notorious groundwater contaminant, frequently detected in sites impacted by industrial wastewater (8).

The use of UV-based AOPs for treating groundwater contaminated with organic chemicals has increased over the last decade. Specifically, UV/H_2O_2 is currently applied in numerous groundwater remediation sites in the US and elsewhere (9–11), mostly for degrading 1,4-dioxane and chlorinated solvents. These proven carcinogenic (or probable carcinogenic) chemicals are considered highly challenging groundwater contaminants, and are a main cause for the closure of water-supply wells all over the world (12–16). In the US for example, the third round of the Unregulated Contaminant Monitoring Rule (UCMR3) detected 1,4-dioxane in approximately 20% of public water systems, which ranked it second among the 28 tested contaminants. In addition, 1,4-dioxane often co-occurred with other chlorinated solvents (17,18).

In the context of UV-AOP application, UV/NO_3^- may present an attractive alternative to UV/H_2O_2, since it makes use of indigenous NO_3^- as a radicals' sensitizer, eliminating the need for the expensive hydrogen peroxide. In addition, NO_3^- is frequently detected in groundwater wells,

as a result of intense agricultural activity, often in parallel to organic contaminants (19–22). An important drawback of UV/NO_3^- is the *in-situ* generation of nitrite (NO_2^-), a harmful by-product of NO_3^- photolysis (3,23). However, previous work showed that concentration of NO_2^- reaches important levels only at high NO_3^- concentrations and extreme UV dose (1), and that it can be controlled through the addition of sulphite and the production of reducing radicals (8).

Kinetic models for contaminants degradation by UV/H_2O_2 have been developed for the vast majority of compounds. These models mostly use the compounds' photochemical properties, background water quality and technical parameters of the UV system, such as H_2O_2 concentration. Alternatively, studies applied bulk parameters such as specific UV absorbance (SUVA) (24), or specific indicators such as sucralose (7), for predicting UV/H_2O_2 effectiveness. Developing analogous indicators for UV/NO_3^- on the other hand was never published, specifically for treating groundwater contaminants. The goals of this study were to (i) determine parameters affecting UV/NO_3^- degradation kinetics of different organic groundwater contaminants, based on their degradation behavior, and (ii) identify a set of metrics and algorithm for predicting the effectiveness of UV/NO_3^- as a groundwater treatment, based on the photochemical properties of a contaminant.

MATERIALS AND METHODS

Chemicals. Ten groundwater contaminants were selected for the study, based on their environmental relevance and photochemical properties (Table 1). Seven chlorinated solvents: Dichloromethane (DCM), 1,2 dichloroethane (DCA), trichloroethene (TCE), perchloroethylene (PCE), 1,1 dichloroethene (DCE), 1,2 dichlorobenzene (DCB) and 1,2,4 trichlorobenzene (TCB); one fuel additive (MTBE), one endocrine disruption compound (Bisphenol A - BPA) and one pesticide (isoproturon). In addition, 1,4 – dioxane and carbamazepine (CBZ) were used for

validation, based on data published previously (5,8). All compounds were analytical grade, purchased from Sigma-Aldrich (Israel). Stock solutions were prepared separately in deionized water (resistance = 18.2 MΩ·cm) at concentrations according to the compound's solubility. High-performance liquid chromatograph (HPLC) - grade solvents and chemicals (acetonitrile, methanol, formic acid, sodium hydroxide) were purchased from Bio-Lab Ltd. (Jerusalem, Israel). All chemicals were used as received.

Photochemical Experiments. UV experiments were performed in a temperature controlled (25°C) 2.5 L glass cylindrical batch reactor (8). The center of the reactor was occupied with a quartz sleeve, housing a 100 W MP UV lamp (Ace-Hanovia, London, UK). Pathlength between quartz sleeve to reactor wall was approximately 3 cm, and the average fluence-rate inside the reactor was measured as 3.4 mW/cm^2, using nitrate actinometry adapted for 200 – 300 nm (25). In a typical experiment, the UV lamp was first turned on for 30 mins for warmup, chemicals were then added to the water and samples were withdrawn at predetermined intervals for analysis. Unless specified otherwise, contaminants were tested separately at initial concentration of 1 mg/L, using phosphate buffer saline (10 mM at pH 7.5), and each irradiation experiment was repeated at least three times.

Analytical Methods. Detection of chlorinated solvents was done with an Agilent 7890 gas chromatograph (GC), equipped with an electron capture detector (ECD) and a 624 UI 30m x 0.25mm, 1.40u column. Prior to GC analysis, samples underwent LLE extraction with n-pentane (EPA Method 551.1, with modifications). Total detection limit for chlorinated solvents (including LLE and GC) was in the range of 5 – 50 µg/L. 1,4-dioxane was analyzed by GC/FID, using DCM for LLE extraction followed by nitrogen evaporation (26). MTBE was detected using a 6890/5973 GC/mass spectrometer (MS) instrument (Agilent). Here, water samples were introduced to the GC using MPS 2 XL twister headspace (Gerstel, Mülheim, Germany) controlled by Maestro software

(v.1.4.11.7, Gerstel). Bisphenol A and carbamazepine were monitored with HPLC-DAD (Agilent 1100, XDB C18 column 4.6 ×150 mm). Molar absorption coefficients were measured using a UV2600 Shimadzu spectrophotometer. Dissolved organic carbon (DOC) was measured using a TOC-VSCH analyzer (Shimadzu Corp., Japan). Nitrate and nitrite were quantified by an ECO Ion Chromatograph (Metrohm, Switzerland).

RESULTS AND DISCUSSION

UV/NO_3^- Degradation of different contaminants. Degradation of all tested compounds by medium pressure UV/NO_3^- followed pseudo-first order kinetics, characteristics of UV/AOPs (27). An example for time-based degradation of three contaminants, exhibiting different degradation behaviors, is presented in Figure 1. Addition of 5 mg/L-N NO_3^- to UV degradation of DCM did not affect its degradation rate (Figure 1a). On the other hand, addition of NO_3^- to UV treatment of PCE and BPA either decreased (for PCE) or increased (for BPA) the compound's degradation rate.

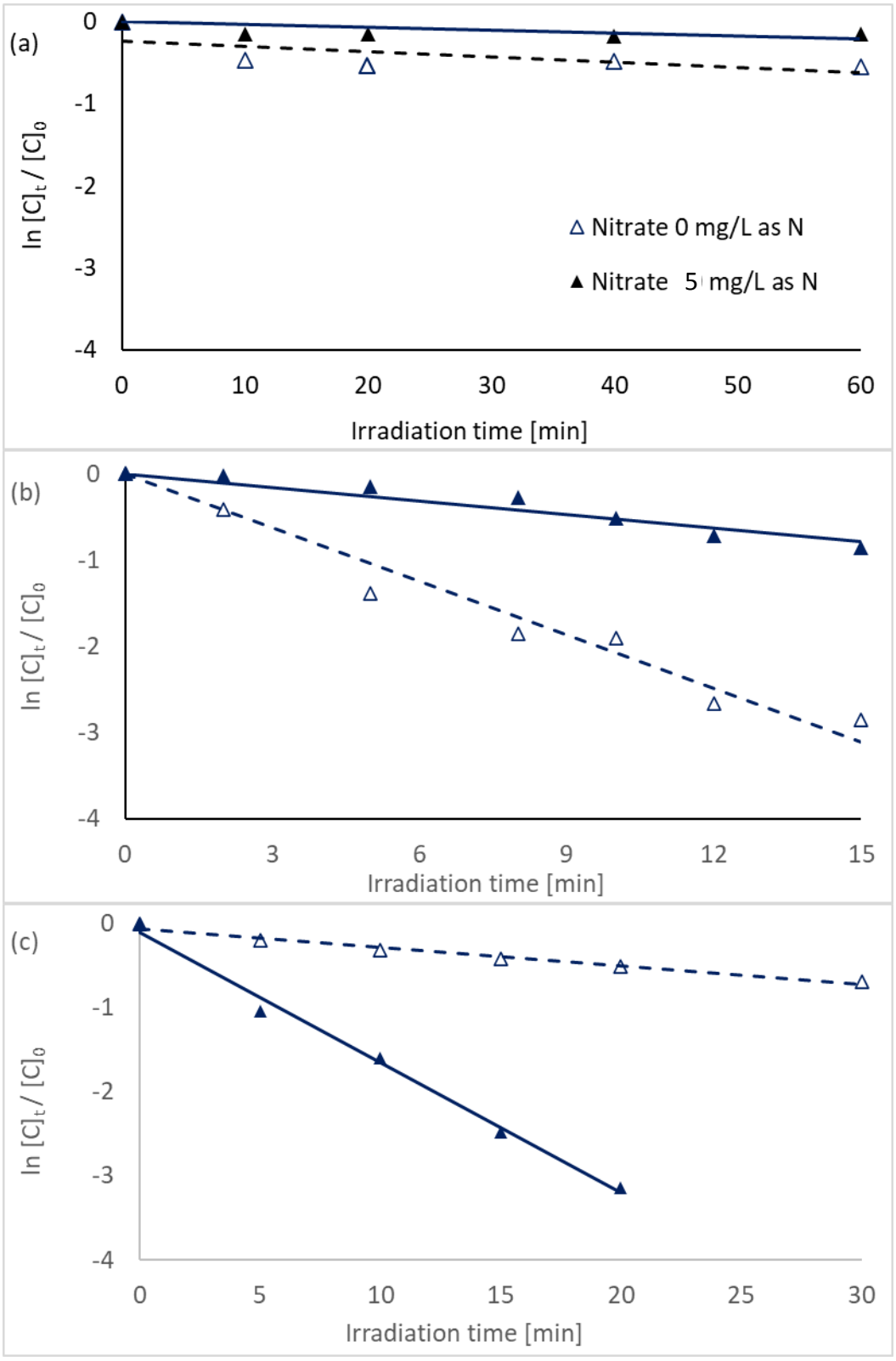

Figure 1. UV degradation of (a) DCM, (b) PCE and (c) BPA, in PBS, without NO_3^- and with at 5 mg/L-N NO_3^-. Notice the different scales of the x-axis.

Three kinetic patterns were also observed when testing the degradation of contaminants at different NO_3^- concentrations, up to 15 mg/L-N (Figure 2). For DCM, increasing NO_3^- concentration up to 15 mg/L-N did not change the degradation rate constant. For PCE, degradation rate decreased rapidly with NO_3^- concentration up to 5 mg/L-N. Further increasing NO_3^- up to 15 mg/L-N had little additional effect. For BPA, the opposite trend was observed, rapid increase in degradation rate with NO_3^- concentration up to 5 mg/L-N, followed by a gradual decrease from 5 to 15 mg/L-N. These observed degradation behaviors can be explained by the compounds' different photochemical properties, as elaborated in the next section.

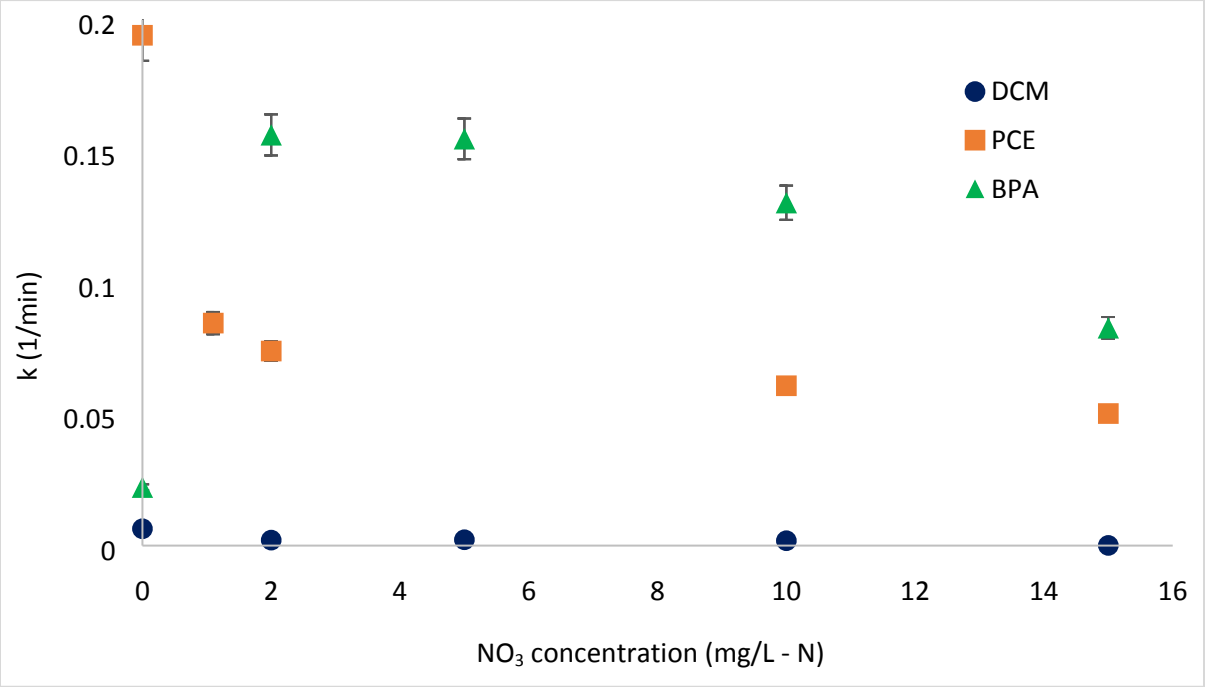

Figure 2. Time-based first order degradation rate constant as a function of NO_3^- concentration for DCM, PCE and BPA.

Photochemical properties of the tested contaminants. Detailed mechanistic and kinetic models for UV/NO_3^- degradation of organic compounds were already described elsewhere (5,28–30). The purpose of this work was to develop simple metrics for predicting the degradability of groundwater

147 contaminants during treatment. For that, a simplified kinetic model was used, dividing degradation
148 into direct- and indirect photolysis, with the later accounting for reactions of contaminants with
149 key photo-sensitized oxidants: •OH and RNS.

150 $$-\frac{d[C]}{dt} = k'_d[C] + \sum_i k_{i,C}[i][C] \qquad (1)$$

151 Here, k'_d is the pseudo first-order photolysis rate constant (1/s), $k_{i,,C}$ is the second-order reaction
152 rate constant of the compound with reactive specie "i" ($M^{-1}s^{-1}$).

153 Direct photolysis depends on light availability (fluence rate inside the reactor; E^P_{avg}, E/s/cm^2) and
154 the photochemical properties of target contaminants, specifically: molar absorption spectrum (ε,
155 $M^{-1}cm^{-1}$) and quantum yield across wavelengths (Φ, mol/E). For UVMP, wavelength-dependent
156 parameters are typically integrated between 200 – 300 nm (31). The factor '1000' in the equation
157 below converts from cm^3 to l.

158 $$k'_d = \Phi \sum_\lambda E^P_{avg}(\lambda)\varepsilon(\lambda) \times \ln(10) \times 1000 \qquad (2)$$

159 Indirect photolysis is more complex, due to the numerous reaction pathways of participating
160 reactive species. For example, at high concentration, photoproduced NO_2^- will react with •OH to
161 produce nitrogen dioxide •NO_2. Both radicals may participate in contaminants degradation during
162 UV/NO_3^- (5). Key parameters affecting indirect photolysis are the concentrations of photo-
163 sensitized oxidants (a function of NO_3^- concentration) and their reaction rate with target
164 contaminants.

165 In general, the presence of low concentrations of NO_3^- during UV treatment of organic
166 contaminants results in two simultaneous effects: (i) photoproduction of radicals, which may
167 increase degradation rate of contaminants and (ii) decrease in available light below 240 nm due to
168 nitrate absorbance, which may slow the contaminant's direct photolysis (and subsequently total

degradation). In addition, at levels higher than 5 mg/L-N, NO_3^- photo-produce significant levels of NO_2^-, which acts as an effective •OH scavenger and $•NO_2$ promoter (5). The total effect of NO_3^- mostly depends on its concentration and photochemical properties of the target contaminant.

Table 1 summarizes relevant photochemical parameters for all tested contaminants. Reaction rate constants with photo-sensitized oxidants were adapted from the scientific literature, and were mostly available for •OH (29,32,33). Molar absorption coefficients are presented for wavelength 223 nm, representing the maximum overlap between lamp emission and NO_3^- absorption spectrum (complete spectrums are provided in Figure S1 in *Supporting Information*). Quantum yields (Φ) for direct photolysis were calculated from photolysis experiments without NO_3^-, using the time-based degradation rates (Equation 2). In addition, fluence-based rate constants were calculated (k_{UV}, cm^2/mJ), by plotting the compounds direct photolysis *vs*. the product of average fluence rate (calculated with actinometry) and time (34).

Table 1. Photochemical parameters of the target contaminants

Compound	$k_{•OH,C}$ $M^{-1}s^{-1}$	$k_{•NO2,C}$ $M^{-1}s^{-1}$	k_{UV} **cm^2/mJ**	ε_{223nm} **1/Mcm**	Φ **mol/E**	ε_{223} x Φ **l/E/cm**
DCM	$5.8x10^7$	NA	$3.1x10^{-5}$	0.08	$3.1x10^{-1}$	0.024
DCA	$^*2.2x10^8$	NA	$3.3x10^{-5}$	7.3	$3.7x10^{-2}$	0.27
TCE	$4.0x10^9$	NA	$8.0x10^{-4}$	1172.9	$7.6x10^{-2}$	89.14
PCE	$2.6x10^9$	NA	$9.5x10^{-4}$	1161.6	$6.7x10^{-2}$	77.83
DCE	$6.2x10^9$	NA	$1.3x10^{-3}$	31.5	$3.6x10^{-1}$	11.34
DCB	$^{**}7.9x10^9$	NA	$2.6x10^{-4}$	12180	$2.6x10^{-3}$	31.67
TCB	$^{**}6.1x10^9$	NA	$2.3x10^{-4}$	7376	$3.6x10^{-3}$	26.55
MTBE	$2.0x10^9$	NA	$2.4x10^{-4}$	14.04	$4.2x10^{-1}$	5.89

BPA	$1.0x10^{10}$	$2.25x10^{4}$	$1.1x10^{-4}$	12918	$3.0x10^{-4}$	3.87
Isoproturon	$3x10^{9}$	NA	$5.5x10^{-4}$	9805	$1.8x10^{-3}$	17.65

*In air, https://inchem.org/documents/ehc/ehc/ehc176.htm#SectionNumber:1.1
**Values for 1,4 dichlorobenzene and 1,2,3 trichlorobenzene
NA-Not available

The data in Table 1 was used to explain the kinetic behaviors in Figure 2. Direct photolysis of DCM is extremely low, with fluence-based rate constant of $k_{UV} = 3.1x10^{-5}$ cm^2/mJ. In addition, its reaction rate with •OH (and likely with other radicals) is in the lower range of •OH reactions ($5.8x10^{7}$ M^{-1}s^{-1}). Subsequently, its degradation during UV/NO_3^- is relatively slow, and marginally affected by increase in photooxidants concentration or decrease in available light (Figure 2). PCE on the other hand has relatively high direct photolysis ($k_{UV} = 9.5x10^{-4}$ cm^2/mJ, Table 1) and high reaction rate with •OH ($k_{•OH,PCE} = 2.6x10^{9}$ M^{-1}s^{-1}). In this case, addition of NO_3^- reduces its direct photolysis and increases indirect photolysis (considering •OH is the dominant photooxidant). Apparently, for PCE, the effect of light screening by NO_3^- dominates over radicals' production, which leads to a decrease in its total degradation rate with addition of NO_3^-. For BPA, direct photolysis is slower than PCE ($k_{UV} = 1.1x10^{-4}$, cm^2/mJ, Table 1), whereas reactions with photooxidants are extremely high. This means that BPA degradation during UV/NO_3^- mostly results from indirect photolysis, and NO_3^- principally acts as a photosensitizer.

For BPA, previous studies concluded that reaction with RNS was the principal path for its degradation during 254 nm UV/NO_3^-, with less than 30% removal attributed to •OH (28). In this case, degradation rate of BPA should increase with NO_3^- over the entire concentration range. The gradual decrease in BPA degradation rate at NO_3^- > 5 mg/l-N (Figure 2) may imply that, under MPUV light, the contribution of •OH is more significant. Under these conditions, photo-produced NO_2^- acts as an •OH scavenger, slowing BPA degradation at high NO_3^- levels. Similar degradation

behavior to BPA was previously observed by Keen (35) for carbamazepine and Lester (8) for 1,4-dioxane. Both compounds are relatively photo-stable, with k_{UV} of 2 x 10^{-4} cm^2/mJ (carbamazepine) and 3.2x10^{-5} cm^2/mJ (1,4-dioxane) (8,36). In addition, reactions of •OH with 1,4-dioxane and carbamazepine are relatively high: 2.8x10^9 $M^{-1}s^{-1}$ (32) and 8.02x10^9 $M^{-1}s^{-1}$ (33) respectively.

Grouping contaminants according to photochemical properties and degradation kinetics. Degradation of all tested compounds followed one of the three kinetic behaviors described in Figure 2 (complete data is given in Figure S2 of the *Supporting Information*). Subsequently, compounds were divided into four groups (Table 2), according to metrics related to direct and indirect photolysis.

Matrices for direct photolysis included: (i) fluence-based photolysis rate (k_{UV}, cm^2/mJ) (31) or (ii) the product of the compounds molar absorption coefficient at 223 nm and MPUV photolysis quantum yield (ε_{223} x Φ, l/E/cm). These parameters are relatively simple to obtain, either by measuring or from the literature, and best represent direct photolysis during MPUV/NO_3^-. The wavelength 223 nm was selected for the second parameter, since it is located at the maximum overlap between NO_3^- absorption and MPUV lamp emission (S1, *Supporting Information*). In other words, light absorption of a contaminant (and subsequently its direct photolysis) will be most affected by the presence of NO_3^- at 223 nm. For indirect photolysis, reaction rate constant with •OH was selected. Despite the fact that •OH is not necessarily the dominant photooxidant in a UV/NO_3^- system, especially in the presence of high levels of carbonates (28), its reaction rate constants are largely available and provide good indication for the susceptibility of a contaminant to electrophilic attack.

By correlating between degradation kinetics and photochemical parameters, we estimated that k_{UV} of approximately 2 x10^{-4} cm^2/mJ and ε_{223} x Φ of ~ 4 l/E/cm separates the photo-stable and

photo-sensitive compounds, in relation to direct photolysis. For indirect photolysis, a threshold of $k_{\bullet OH,C} = 1x10^9$ $M^{-1}s^{-1}$ was set for high and low reactive compounds (32,33). A detailed explanation for each group is given below.

Table 2. Grouping of contaminants according to their photochemical properties and NO_3^- degradation kinetics

Group	UV parameter	$k_{\bullet OH,C}$ $M^{-1}s^{-1}$	Compound
I	Photo-stable: $k_{UV} < 2\ x10^{-4}$ cm^2/mJ or $\varepsilon_{223} \times \Phi < 4$ 1/M cm	Slow •OH reaction: $k_{\bullet OH,C} < 1x10^9$	DCM, DCA
II	Photo-sensitive: $k_{UV} > 2\ x10^{-4}$ cm^2/mJ or $\varepsilon_{223} \times \Phi > 4$ 1/M cm	Fast •OH reaction: $k_{\bullet OH,C} > 1x10^9$	TCE, PCE, DCE, DCB, TCB, MTBE, Isoproturon
III	Photo-stable: $k_{UV} \leq 2\ x10^{-4}$ cm^2/mJ or $\varepsilon_{223} \times \Phi < 4$ 1/M cm	Fast •OH reaction: $k_{\bullet OH,C} > 1x10^9$	BPA Carbamazepine 1,4-dioxane
IV	Photo-sensitive: $k_{UV} > 2\ x10^{-4}$ cm^2/mJ or $\varepsilon_{223} \times \Phi > 4$ 1/M cm	Slow •OH reaction: $k_{\bullet OH,C} < 1x10^9$	N/A

Group I - photo-stable compounds with slow •OH reaction. Photolysis of these compounds is not affected by the presence of NO_3^-; *Group II* - high direct photolysis (photo-sensitive) and fast reaction with •OH. The presence of NO_3^- during UV treatment of compounds in this group either has little effect or decreases their degradation rate, since NO_3^- is a highly effective light absorber, which dominates over its role as a radicals' promoter (detailed calculation is provided in *Supporting Information*). In addition, NO_3^- at concentrations > 5 mg/L-N indirectly scavenges •OH, through production of NO_2^- (5). *Group III* - photo-stable and fast •OH reacting compounds.

In this case, NO_3^- at concentrations ≤ 5 mg/L – N increases the compounds' UV degradation rate, since NO_3^- mainly acts as a radicals' promoter. At higher NO_3^- concentrations, degradation rates of compounds degraded by •OH will stabilize or even decrease, following the formation of NO_2^- at significant levels, whereas degradation rate of contaminants reactive to RNSs is expected to further increase. Carbamazepine and 1,4 – dioxane belong to *Group III,* with k_{UV} of 1.2 x10^{-4} cm^2/mJ and ε_{225} x Φ of 2.15 (carbamazepine), and 2.8 x 10^{-5} cm^2/mJ and 3.23 l/E/cm (1,4 – dioxane).

Evidently, a fourth group exists - *Group IV* - with compounds exhibiting high direct photolysis and slow •OH reaction (none of the tested compounds belonged to this group). Based on the kinetics behavior of Group II, it is reasonable to assume that the presence of NO_3^- in water during UV treatment of *Group IV* compounds will slow their degradation due to light screening. An example for a water contaminant belonging to *Group IV* is N-nitrosodimethylamine (NDMA), with $k_{\bullet OH,NDMA}$ = 3.3x10^8 M^{-1} s^{-1} (33), k_{UV} of 2.4 x10^{-3} cm^2/mJ and ε_{225} x Φ of approximately 2100 (37).

A somewhat different grouping was proposed by Huang et al. (28), which classified organic contaminants into three groups, based on the contributions of direct UV and sensitized oxidants to their degradation during LPUV/NO_3^- (254 nm) treatment of carbonates-containing water. Their groups included photo-sensitive compounds, degraded mainly by direct photolysis at 254 nm and RNS, photostable compounds degraded mostly by RNS and, photostable compounds degraded mostly by •OH. They concluded that degradation of the third group will be ineffective in the presence of high concentrations of HCO_3^- (183 mg/L) due to •OH scavenging (using 254 nm UV source). The grouping in our case is based on NO_3^- sensitization by MP UV, which is much more effective than LP for producing photooxidants.

Implication for field-scale treatment. The discussion above implies that UV/NO_3^- can be effective for both Group II and Group III contaminants. For Group II, the presence of NO_3^- will simultaneously slow direct photolysis and enhance indirect photolysis. However, the compounds' high reaction rates with photoproduced oxidants are expected to keep their overall degradation rate relatively high. Subsequently, this section will focus solely on these two groups, evaluating the full-scale application of UV/NO_3^-, specifically: (i) The cost-effectiveness of the treatment, (ii) formation of NO_2^- and (iii) the impact of background water constituents.

To address the first point, we used the E_{EO} parameter (electrical energy per order, kWh/m^3/order), often employed for assessing the cost-effectiveness of AOPs (Equation 5) (38).

$$E_{EO} = \frac{P \times t \times 1000}{V \times 60 \times \log\left(\frac{C_0}{C_t}\right)} = \frac{38.4 \times P}{V \times k} \qquad (5)$$

Where, P is the lamp power (kW), V is the volume of treated water (l), C_0 and C_t are the initial and final concentrations of the contaminant, and k is the first-order rate constant (1/min) for the compound's overall decay under the tested conditions.

Table 3 summarizes the E_{EO} values for degrading Group II & III contaminants, for NO_3^- concentrations of 0 (direct photolysis), 2 and 5 mg/L – N. Higher NO_3^- levels generally did not further enhance the compounds' degradation rate and were therefore not evaluated. As expected from Figure 2 (and S2), the electrical cost of Group III contaminants was reduced in the presence of NO_3^- by up to 7-fold (for BPA) and increased for contaminants from Group II (compared to UV alone). To exemplify the full-scale implications of Table 3, we hypothesize a treatment of groundwater contaminated with 1 mg/L BPA and 2 mg/L-N of NO_3^-. If the treatment's goal is 10 μg/L BPA, electrical energy will be approximately 19.6 kWh/m^3. Considering the cost of

electricity at \$0.12 per kWh (Israel Electric Company), the treatment's cost attributed to electricity will be \$2.35 per m^3.

Table 3. Electrical energy per order (E_{EO}, kWh/m^3/order) for compounds in Groups II&III

Initial NO_3^- concentrations		0 mg/L- N	2 mg/L- N	5 mg/L- N
Compound	**Group**	E_{EO} (kWh/m^3/order)		
TCE	II	9.8	33.8	46.9
PCE		8.2	21.6	25.7
DCE		5.9	28.1	26.7
DCB		25.9	49.2	100.9
TCB		26.9	50.9	103.5
MTBE		34.4	124.0	160.0
Isoproturon		13.3	20.0	27.4
BPA	III	72.7	9.8	10.1
CBZ		80.0	18.4	17.8
1,4 - dioxane		622.5	212.5	221.3

Comparing the date in Table 3 to the scientific literature is not straight forward, since E_{EO} is largely system-dependent, influenced by parameters such as the type and size of the reactor and water quality. Miklos et al. (39) critically reviewed E_{EO}s from large number of AOPs studies, dividing them into different categories to reduce variability. For photo-stable contaminants and lab-scale UV/H_2O_2 systems, they found E_{EO} in the range of 0.1 - 10 kWh/m^3/order. A different study by Rosenfeldt and Linden (34) examined UV/H_2O_2 degradation of BPA in a collimated beam reactor, and showed that addition of 15 mg/L H_2O_2 increased its degradation rate by 6-fold (compared to UV alone), similar to our data. We can therefore conclude that UV/NO_3^- can be competitive with

294 UV/H_2O_2 (and other UV-AOPs), depending on the target contaminant and, especially when
295 considering the additional cost of H_2O_2 and a complementary H_2O_2 quenching system.

296 Another barrier for UV/NO_3^- application is the photogeneration of NO_2^-, a harmful
297 byproduct with U.S. EPA drinking water standard of 1 mg/L-N - lower than nitrate (10 mg/L-N)
298 (www.epa.gov). Formation of NO_2^- mostly depends on the initial concentration of NO_3^- and on
299 UV exposure at wavelengths below 240 nm (1). Figure 3 presents the formation rate of NO_2^- during
300 UV/NO_3^- as function of applied electrical energy, for initial NO_3^- concentrations of 2, 5 and 10
301 mg/L-N. Concentration of NO_2^- reached EPA standard after 238 and 98 kWh/m^3, for 5 and 10
302 mg/L-N NO_3^- respectively. For 2 mg/L-N NO_3^-, nitrite formation could not reach US EPA NO_2^-
303 standards. Applying this data to Table 3, while considering a typical removal target of two orders
304 of magnitude, suggests that: (i) under high NO_3^- levels of 10 mg/L-N, removal of most compounds
305 approach or surpass NO_2^- standard; hence these conditions may be considered unsafe. (ii) At lower
306 NO_3^- levels ($\leq$ 5 mg/L-N), many of Groups II & III contaminants can be safely degraded, with
307 some exceptions such as MTBE (Group II) and 1,4-dioxane (Group III). Therefore, Groups II &
308 III should be narrowed to include only contaminants with the highest degradation rate, which
309 would allow safe and efficient degradation during UV/NO_3^-.

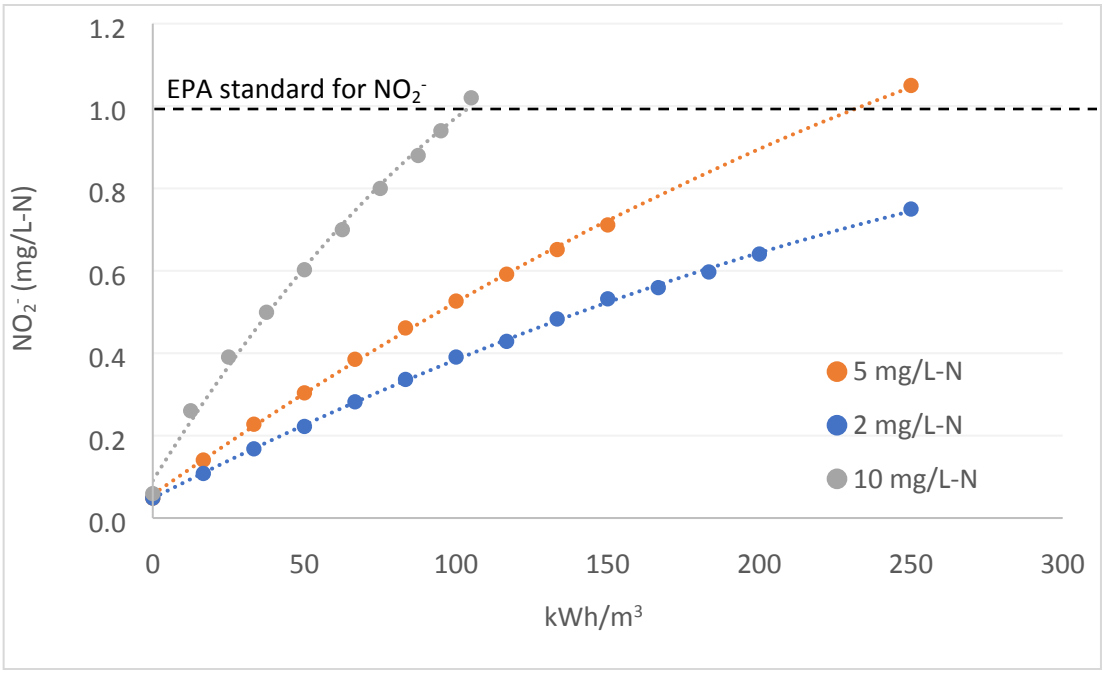

Figure 3. Formation of NO_2^- as function of applied electrical energy, for different initial NO_3^- concentrations.

Subsequently, we defined two additional groups: II' & III'. For precaution measures we identified 200 kWh/m^3 as the safety threshold for two orders of magnitude removal. Compounds requiring higher energy level (Table 3) were considered unsafe for removal. Under this condition, Group III' included (photostable) compounds with extremely fast reaction with •OH ($k_{•OH}$ > 8 x 10^9 M^{-1}s^{-1}): CBZ and BPA in our case. Group II' includes compounds in the upper range of direct photolysis (k_{UV} > 5 cm^2/mJ or ε_{223} x Φ > 10 l/E/cm) and high •OH reaction ($k_{•OH}$ > 1 x 10^9 M^{-1}s^{-1}). In our case, PCE, TCE, DCE and isoproturon (Table 2).

The last point relates to the impact of key groundwater constituents, specifically, bicarbonate (HCO_3^-) and natural organic matter (NOM). For that, we tested UV/NO_3^- degradation of representative contaminants - CBZ (Group III') and isoproturon (Group II'), with and without the addition of HCO_3^- (180 mg/L) and fulvic acid (2.5 mgC/L), a commonly used NOM standard. Irradiations were carried out with 5 mg/L-N of NO_3^- and a mixture of the two contaminants (0.5 mg/L each).

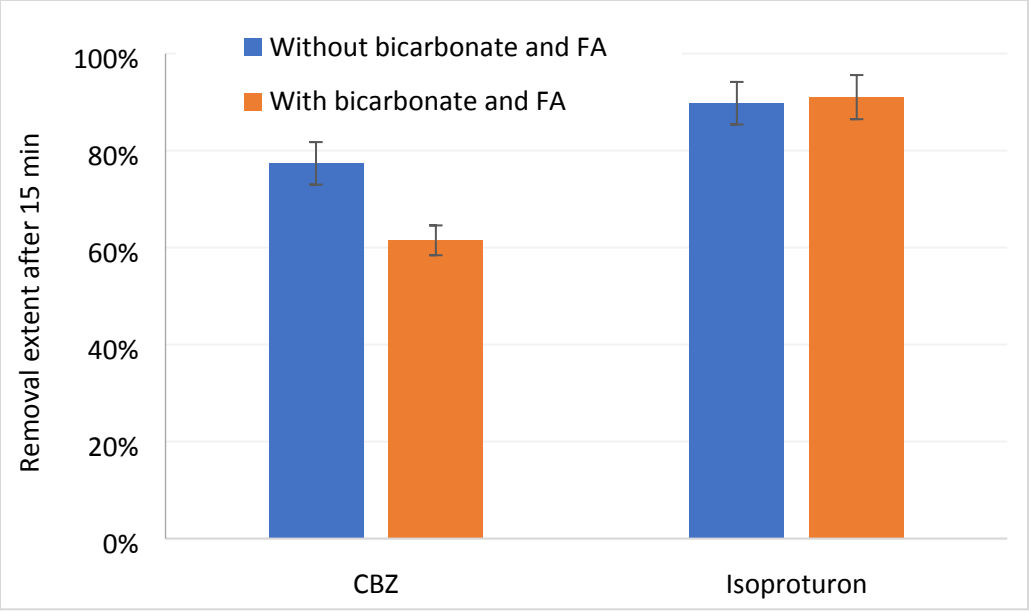

Figure 4. Removal extent of CBZ and isoproturon after 15 min of UV/NO_3^- (5 mg/L-N), with and without HCO_3^- and FA at 180 mg/L and 2.5 mgC/L respectively.

Addition of HCO_3^- and fulvic acid slowed the degradation rate of CBZ by approximately 20% but didn't affect the degradation of isoproturon (Figure 4). At the tested concentrations (characteristics for groundwater), HCO_3^- and fulvic acid mainly act as •OH scavengers, with minor contribution to light screening (Figure S4). This can explain their adverse effect on CBZ (and Group III' chemicals in general), which are principally degraded through reactions with photooxidants, including •OH. For contaminants with significant degradation paths other than •OH (e.g. isoproturon), this slowing effect is expected to be less significant, or even reversed to accelerate degradation, through the formation of carbonate radicals (28).

Finally, we propose a simplified decision tree to predict if a groundwater contaminant will be safely degraded during MPUV/NO_3^- (Figure 5).

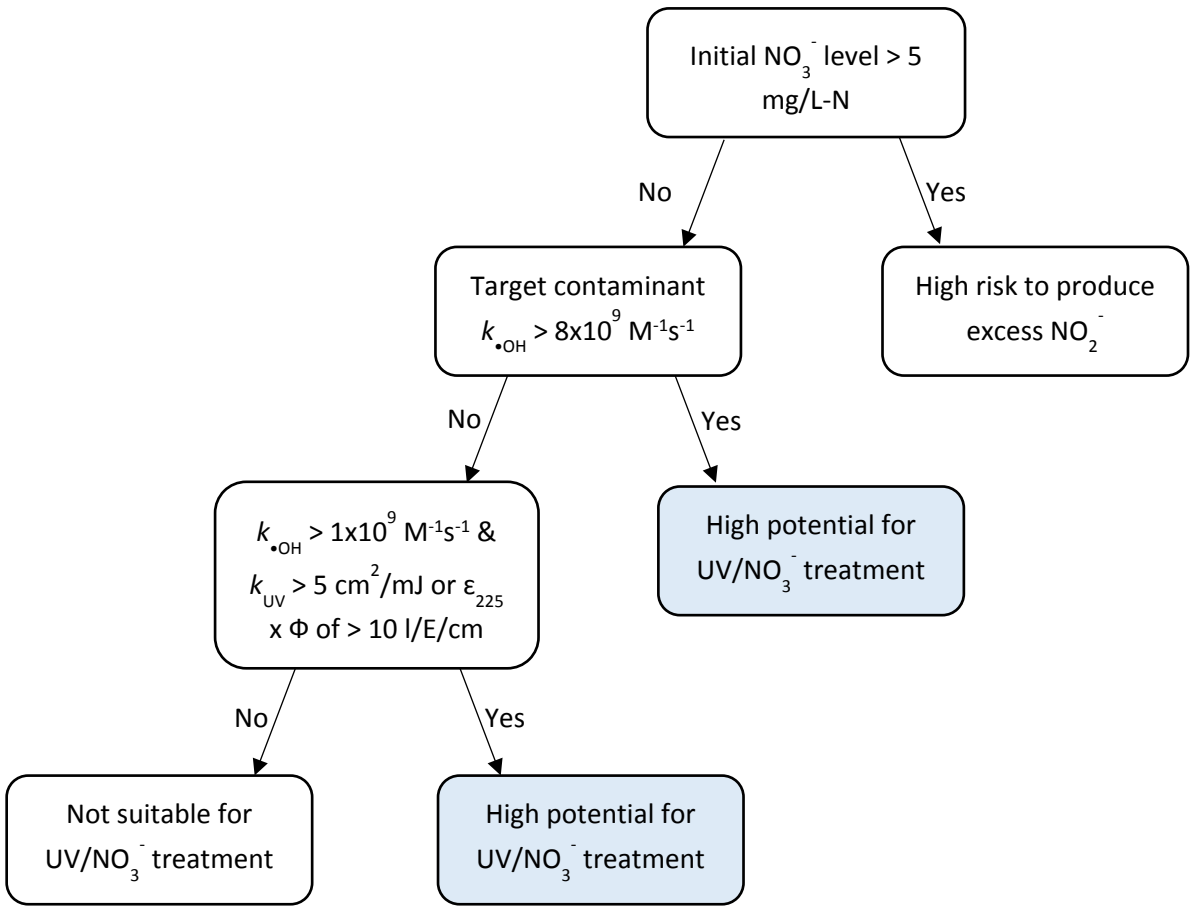

Figure 5. A decision tree to determine the suitability of contaminants to UV/NO_3^- treatment

Author contributions

Lidori Edri and Nadeem Ibrahim: Conceptualization, Methodology, Investigation; Karl Linden: Visualization; Dror Avisar and Aviv Kaplan: Investigation; Sara Hayoune: Methodology; Yaal Lester: Writing- Reviewing and Editing.

Acknowledgments

This work was supported by National Science Foundation-BiNational Science Foundation (NSF-BSF) Award CBET- 2019615.

Supporting Information. Spectrum of medium pressure Hg lamp with molar absorption spectrum of NO_3^-, degradation rate constants for the tested compounds as function of NO_3 concentration, a model for the impact of NO_3^- on UV degradation of Group II contaminants.

References

1. Sharpless CM, Linden KG. UV photolysis of nitrate: Effects of natural organic matter and dissolved inorganic carbon and implications for UV water disinfection. Environ Sci Technol. 2001;35(14):2949–55.

2. Sharpless CM, Seibold DA, Linden KG. Nitrate photosensitized degradation of atrazine during UV water treatment. Aquat Sci. 2003;65(4):359–66.

3. Mack J, Bolton JR. Photochemistry of nitrite and nitrate in aqueous solution: A review. J Photochem Photobiol A Chem. 1999;128(1–3):1–13.

4. Scholes RC. Emerging investigator series: contributions of reactive nitrogen species to transformations of organic compounds in water: a critical review. Environ Sci Process Impacts. 2022;24(6):851–69.

5. Keen OS, Love NG, Linden KG. The role of effluent nitrate in trace organic chemical oxidation during UV disinfection. Water Res. 2012;46(16):5224–34.

6. Payne EM, Liu B, Mullen L, Linden KG. UV 222 nm Emission from KrCl∗ Excimer Lamps Greatly Improves Advanced Oxidation Performance in Water Treatment. Environ Sci Technol Lett. 2022;9(9):779–85.

7. Lester Y, Ferrer I, Thurman EM, Linden KG. Demonstrating sucralose as a monitor of full-scale UV/AOP treatment of trace organic compounds. J Hazard Mater [Internet].

2014;280:104–10. Available from: http://dx.doi.org/10.1016/j.jhazmat.2014.07.009

8. Lester Y, Dabash A, Eghbareya D. UV Sensitization of Nitrate and Sulfite : A Powerful Tool for Groundwater Remediation. 2018;

9. SCDOH. 1 , 4-Dioxane in our Water Resources – Fact Sheet. 2015;(June):1–3.

10. Cortez CAE. Agenda Background Program Approach Remediation Projects Funding Next Steps. 2016.

11. Biggs J. Tucson Water Tackles 1 , 4-dioxane & PFAS Challenges within TCE CERCLA Program. 2021.

12. Jackson RE. Anticipating Ground-Water Contamination by New Technologies and Chemicals : The Case of Chlorinated Solvents in California. 2016;(April).

13. Matteucci F, Ercole C, Gallo M. A study of chlorinated solvent contamination of the aquifers of an industrial area in central Italy : a possibility of bioremediation. 2015;6(September):1–10.

14. Manamsa K, Crane E, Stuart M, Talbot J, Lapworth D, Hart A. Science of the Total Environment A national-scale assessment of micro-organic contaminants in groundwater of England and Wales. Sci Total Environ [Internet]. 2016;568:712–26. Available from: http://dx.doi.org/10.1016/j.scitotenv.2016.03.017

15. Rivett MO, Turner RJ, Glibbery P, Cuthbert MO. The legacy of chlorinated solvents in the Birmingham aquifer , UK : Observations spanning three decades and the challenge of future urban groundwater development. J Contam Hydrol [Internet]. 2012;140–141:107–23. Available from: http://dx.doi.org/10.1016/j.jconhyd.2012.08.006

16. Dyksen JE, Hess AF. Alternatives controlling organics in groundwater supplies. 1982;

17. Adamson DT, Mahendra S, Walker KL, Rauch SR, Sengupta S, Newell CJ. A Multisite Survey to Identify the Scale of the 1,4-Dioxane Problem at Contaminated Groundwater Sites. Environ Sci Technol Lett. 2014;1(5):254–8.

18. Adamson DT, Piña EA, Cartwright AE, Rauch SR, Anderson RH, Mohr T, et al. 1 , 4-Dioxane drinking water occurrence data from the third unregulated contaminant monitoring rule. Sci Total Environ [Internet]. 2017;596–597:236–45. Available from: http://dx.doi.org/10.1016/j.scitotenv.2017.04.085

19. Squillace PJ, Scott JC, Moran MJ, Nolan BT, Kolpin DW. VOCs, pesticides, nitrate, and their mixtures in groundwater used for drinking water in the United States. Environ Sci Technol. 2002;36(9):1923–30.

20. Shalev N, Burg A, Gavrieli I, Lazar B. Nitrate contamination sources in aquifers underlying cultivated fields in an arid region - The Arava Valley, Israel. Appl Geochemistry [Internet]. 2015;63:322–32. Available from: http://dx.doi.org/10.1016/j.apgeochem.2015.09.017

21. Burow KR, Nolan BT, Rupert MG, Dubrovsky NM. Nitrate in groundwater of the United States, 1991 - 2003. Environ Sci Technol [Internet]. 2010;44(13):4988–97. Available from: http://dx.doi.org/10.1021/es100546y

22. Haran M, Samuels R, Uri Mingelgrin SG. Quality indicators of the state of chemical pollution in Israel. Isr J Chem. 2002;42:119–32.

23. Wu Y, Bu L, Duan X, Zhu S, Kong M, Zhu N, et al. Mini review on the roles of

nitrate/nitrite in advanced oxidation processes: Radicals transformation and products formation. J Clean Prod [Internet]. 2020;273:123065. Available from: https://doi.org/10.1016/j.jclepro.2020.123065

24. Rosario-Ortiz FL, Wert EC, Snyder SA. Evaluation of UV/H2O2 treatment for the oxidation of pharmaceuticals in wastewater. Water Res [Internet]. 2010;44(5):1440–8. Available from: http://dx.doi.org/10.1016/j.watres.2009.10.031

25. Goldstein S, Rabani J. Actinometers Based on NO 3 - and H 2 O 2 Excitation : Applications for Industrial Photoreactors. Environ Sci Technol. 2008;42(3):3248–53.

26. Park YM, Pyo H, Park SJ, Park SK. Development of the analytical method for 1,4-dioxane in water by liquid-liquid extraction. Anal Chim Acta. 2005;548(1–2):109–15.

27. Rosenfeldt EJ, Melcher B, Linden KG. UV and UV/H2O2 treatment of methylisoborneol (MIB) and geosmin in water. J Water Supply Res Technol - AQUA. 2005;54(7):423–34.

28. Huang Y, Kong M, Westerman D, Xu EG, Coffin S, Cochran KH, et al. Effects of HCO_3^- on Degradation of Toxic Contaminants of Emerging Concern by UV/NO_3^-. Environ Sci Technol. 2018 Oct;

29. Li Y, Wang L, Xu H, Lu J, Chovelon JM, Ji Y. Direct and nitrite-sensitized indirect photolysis of effluent-derived phenolic contaminants under UV254irradiation. Environ Sci Process Impacts. 2022;24(1):127–39.

30. Vinge SL, Shaheen SW, Sharpless CM, Linden KG. Nitrate with benefits: Optimizing radical production during UV water treatment. Environ Sci Water Res Technol. 2020;6(4):1163–75.

442 31. Stefan MI, Bolton JR. Fundamental approach to the fluence-based kinetic and electrical
443 energy efficiency parameters in photochemical degradation reactions: Polychromatic light.
444 J Environ Eng Sci. 2005;4(SUPPL. 1):13–8.

445 32. Buxton G V., Greenstock CL, Helman WP, Ross AB. Critical Review of rate constants for
446 reactions of hydrated electrons, hydrogen atoms and hydroxyl radicals (·OH/·O−in
447 Aqueous Solution. J Phys Chem Ref Data. 1988;17(2):513–886.

448 33. Wols BA, Hofman-Caris CHM. Review of photochemical reaction constants of organic
449 micropollutants required for UV advanced oxidation processes in water. Water Res
450 [Internet]. 2012;46(9):2815–27. Available from:
451 http://dx.doi.org/10.1016/j.watres.2012.03.036

452 34. Rosenfeldt EJ, Linden KG. Degradation of endocrine disrupting chemicals bisphenol A,
453 ethinyl estradiol, and estradiol during UV photolysis and advanced oxidation processes.
454 Environ Sci Technol. 2004;38(20):5476–83.

455 35. Keen OS, Baik S, Linden KG, Aga DS, Love NG. Enhanced biodegradation of
456 carbamazepine after UV/H2O2advanced oxidation. Environ Sci Technol.
457 2012;46(11):6222–7.

458 36. Lester Y, Mamane H, Avisar D. Enhanced removal of micropollutants from groundwater,
459 using pH modification coupled with photolysis. Water Air Soil Pollut. 2012;223(4):1639–
460 47.

461 37. Sharpless CM, Linden KG. Interpreting collimated beam ultraviolet photolysis rate data in
462 terms of electrical efficiency of treatment. J Environ Eng Sci. 2005;4(SUPPL. 1).

463 38. Cater SR, Stefan MI, Bolton JR, Amiri AS. UV/H 2 O 2 Treatment of Methyl. Environ
464 Sci Technol. 2000;34(4):659–62.

465 39. Miklos DB, Remy C, Jekel M, Linden KG, Drewes JE, Hübner U. Evaluation of advanced
466 oxidation processes for water and wastewater treatment – A critical review. Water Res.
467 2018;139:118–31.

468